

Dynamic modelling and simulation of a post-combustion CO₂ capture process for coal-fired power plants

Jianlin Li, Ti Wang, Pei Liu (✉), Zheng Li

State Key Lab of Power Systems, International Joint Laboratory on Low Carbon Clean Energy Innovation, Department of Energy and Power Engineering, Tsinghua University, Beijing 100084, China

© Higher Education Press 2021

Abstract Solvent-based post-combustion capture technologies have great potential for CO₂ mitigation in traditional coal-fired power plants. Modelling and simulation provide a low-cost opportunity to evaluate performances and guide flexible operation. Composed by a series of partial differential equations, first-principle post-combustion capture models are computationally expensive, which limits their use in real time process simulation and control. In this study, we propose a first-principle approach to develop the basic structure of a reduced-order model and then the dominant factor is used to fit properties and simplify the chemical and physical process, based on which a universal and hybrid post-combustion capture model is established. Model output at steady state and trend at dynamic state are validated using experimental data obtained from the literature. Then, impacts of liquid-to-gas ratio, reboiler power, desorber pressure, tower height and their combination on the absorption and desorption effects are analyzed. Results indicate that tower height should be designed in conjunction with the flue gas flow, and the gas-liquid ratio can be optimized to reduce the reboiler power under a certain capture target.

Keywords CO₂ capture, post-combustion capture, simulation, dominant factor

1 Introduction

Improving energy efficiency, developing alternative energy sources, and CO₂ capture and storage (CCS) are the main approach to reduce CO₂ emissions. Different from the alternative energy, CCS combined with fossil fuel power plants will provide a reliable and sustainable power

supply to the grid [1]. As a carbon capture method, Deployment with less reconstruction and modification on power plant, post-combustion capture (PCC) has great potential to reduce CO₂ emissions from existing coal-fired power plants. According to data from China Electricity Council, at the end of 2019, the installed capacity of coal fired power plants built within 10 years in China reached 509 GW, accounting for 43% of total coal fired power installed capacity. These young power plants make them the most likely candidates for PCC technology. In PCC technology, the chemical absorption based on alcohol amine solution is most widely used, of which the general system structure is shown in Fig. 1. Over constant development of solvent-based PCC technologies, industry has gained excellent experience and sufficient confidence to commercialize solvent based technologies in PCC processes [2].

Although solvent-based PCC is regarded as the most promising technology for power plant CO₂ capture, it's commercial deployment still faces two main challenges: (1) As the share of renewable energy increases, the load of coal-fired power plant would change more frequently [3], which means that PCC plants are forced to operate in a flexible manner to follow these changes. (2) Due to the large amount of flue gas to be processed, the PCC plant consumes a lot of energy [4], especially the energy consumption in the reboiler, which accounts for 80% of the capture process [5], leading to a capture cost of 30–40 US \$/tonne. Flexible operation is one of the effective ways to reduce the economic penalty, which can increase operating profit by up to 10% [6]. Achieving smooth flexible operation and integrating with power plant depend on in-depth understanding of the dynamic behavior of the PCC process. Compared with carrying out dynamic experimental studies, dynamic modeling and simulation provide a more cost-effective way to conduct the dynamic performance research.

In general, the PCC dynamic model can be divided into

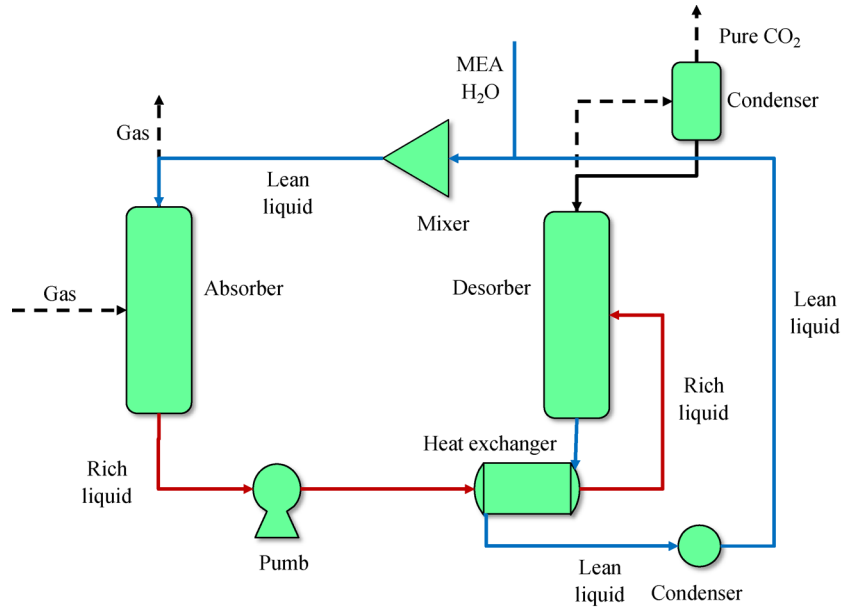


Fig. 1 Structure of a chemical absorption system.

first-principle models and data-driven models. Due to the data-driven nature, data-driven models are simple in structure and efficient in calculation, but limited by the high-quality dynamic data, only a few models were identified from operating data, others were developed based on the data obtained from simulators [7]. Compared with data-driven models, first-principle models can reflect the internal status and better portray the dynamics of PCC process. Fundamentally, first-principle models are based on the separation processes developed decades ago [8], and are established by equilibrium or rate-based methods [9]. The equilibrium method assumes infinitely fast mass transport between liquid and gas, considering chemical reaction kinetics could help improve model accuracy, but it is still difficult to accurately reflect the dynamic behaviors. At present, rate-based approaches considering mass transfer kinetics are widely used in dynamic modeling. After many years of development and improvement, rate-based dynamic models have become mature in methods and theory. Early studies started from separate absorber modelling [10–13] and desorber modelling [14,15], which cannot represent the dynamic behavior of the whole PCC process due to high integration between these two equipment. Nearly at the same time, some studies developed models of whole PCC plants [16,17]. With PCC modeling becoming mature, current research mainly focuses on integration of PCC and power plants [18–20], control strategy [21–23] and process intensification [24,25].

However, these models still cannot be used for online simulation purposed due to the following reasons. Firstly, coverage of working conditions needs to be extended. Many researches deal with the regular operation of PCC

plants, without considering start-up and shutdown processes [26,27]. Kvamsdal [10], Jayarathna [11], and Gaspar [28] developed a rate-based packed column model that can be used to study the start-up process, but the heating-up process in the desorber is not considered in these models, which is essential for the dynamic thermal response in the start-up and shutdown process. Secondly, most existing models are developed on specially software platforms, such as gPROMS, Aspen Plus Dynamics, and UniSim [7,29]. This greatly limits their potential to be used for online simulation purposes, which requires integration with other parts of a power plant. Thirdly, complexity of these models needs to be reduced for real-time simulation and control [7,30], whilst accuracy should be maintained above a certain level. In order to facilitate the calculation, a hybrid modelling method, which develops the basic physical model based on first-principle, and then uses a data-driven approach to fine tune model parameters, may also enable more accurate and efficient calculation of PCC performances, reliability and flexibility.

In this study, we use a hybrid modeling method to develop a whole process dynamic PCC simulator, where data obtained from an Aspen Plus model [31] are fitted using a dominated factor method. Model output at steady state and trend at dynamic state are validated using experimental data obtained from the literature. We then illustrate changes of capture rate at varying process design and operation parameters, covering gas-liquid ratio, reboiler power, desorber pressure, and tower heights. Analysis of energy consumption under these conditions and a capture rate of 90 percent is also conducted. The objective and novelty of this study are to (a) reduce computational expense of dynamic PCC models, making

real-time simulation and complex control strategy possible, (b) establish a whole process dynamic monoethanolamine-based PCC model, which is platform-free and can be easily integrated with a power plant simulator established on different platforms, and (c) analyze impacts of key operating parameters and guide flexible operation of a PCC plant.

2 Modeling and validation

This section presents a dynamic model for the monoethanolamine-based PCC process. Developed by hybrid modeling method, the packed column models are capable for real-time CO₂ absorption and desorption calculation. In order to preheat the rich liquid flowing out of absorber, heat exchangers are developed by shell and tube heat exchanger model. In addition, condensers, coolers, pumps are also indispensable, and briefly modeled. All these models of each unit have been integrated to form dynamic model for the whole PCC process. In this paper, we mainly introduce the hybrid modeling of absorber and desorber.

2.1 Hybrid modeling of physical diffusion and chemical reactions

Both physical diffusion and chemical reactions are essential for the CO₂ absorption and desorption, which leads to complex packed column models. The most rigorous models are developed with many partial differential equations for mass transfer along bulk flow and between the two phases, typically resulting in high-order models. To reduce the complexity of packed column models, replacing rigorous mass transfer by semi-empirical algebraic correlations is generally accepted. In addition, fitting key chemical parameters by dominant factor method, rather than considering the rigorous ion system, can also significantly reduce computing demand. High accuracy is rather a matter of a good data fit than model complexity [30]. In this study, the fitting data come from a validated Aspen Plus model [31], and the formula required for parameters calculation is obtained.

Without chemical reaction happens, physical diffusion will dominant CO₂ mass transfer. CO₂ concentration gradient between liquid and gas phases will causing the CO₂ to diffuse into or out the absorbent. The driving force (DF) is mainly determined by the partial pressure of CO₂ in the gas phase P_{CO_2} and the equilibrium pressure of the

dissolved CO₂ $P_{CO_2}^*$. $P_{CO_2}^*$ is determined by the liquid phase equilibrium CO₂ concentration $[CO_2]^*$ and the CO₂ Henry coefficient in liquid $h_{CO_2,L}$. These equations are as follows:

$$DF = P_{CO_2} - P_{CO_2}^*, \quad (1)$$

$$h_{CO_2,L} = \frac{P_{CO_2}^*}{[CO_2]^*}. \quad (2)$$

Taking the absorption process as example, the formula for calculating CO₂ absorption rate N_{CO_2} is as follows [32]:

$$N_{CO_2} = K_G(P_{CO_2} - P_{CO_2}^*), \quad (3)$$

$$\frac{1}{K_G} = \frac{1}{k_L^*} + \frac{1}{k_G}, \quad (4)$$

where K_G is the total mass transfer coefficient, k_L^* is the unreacted mass transfer coefficient on the liquid side, and k_G is the mass transfer coefficient on the gas side.

Compared with the liquid-side mass transfer coefficient, the gas-side mass transfer coefficient can be ignored [33]. k_L^* [34] and N_{CO_2} can be written as

$$k_L^* = 0.0051 \left(\frac{\mu_1 g}{\rho_1} \right)^{1/3} \left(\frac{\rho_1 \mu_1}{a_e \mu_1} \right)^{2/3} \left(\frac{\mu_1}{\rho_1 D_{CO_2,1}} \right)^{-0.5} (6(1-\varepsilon))^{0.4}, \quad (5)$$

$$N_{CO_2} = \frac{P_{CO_2} - \frac{P_{CO_2}^*}{H_{CO_2,MEA}}}{\frac{1}{k_L^*}} = k_L^* \left(P_{CO_2} - \frac{P_{CO_2}^*}{H_{CO_2,MEA}} \right). \quad (6)$$

When considering CO₂ absorption and desorption, the physical diffusion of CO₂ is accelerated. Enhancement factor E is used to describe this phenomenon, which is a function of CO₂ chemical reaction rate in the liquid phase. For the absorption and desorption, enhancement factor E is respectively calculated by [35],

$$E_{ab} = \frac{\sqrt{D_{CO_2,L} k [RNH_2]}}{k_L^*}, \quad (7)$$

$$E_{de} = 1 + \frac{\left(\frac{D_{RNHCO_2^-,L} \sqrt{K} [RNH_2]}{D_{CO_2,L}} \right)}{\left(1 + 2D_{RNHCO_2^-,L} \sqrt{\frac{K [RNH_3^+]}{D_{RNH_2,L}}} \right) \left(\sqrt{[CO_2]^*} + \sqrt{[CO_2]} \right)}, \quad (8)$$

$$k_{2,MEA} = 9.56 \times 10^8 \exp\left(\frac{-3802.4}{T}\right), \quad (9)$$

where $[RNH_2]$ is the free amine concentration, and k is the reaction rate constant for the reaction of CO₂ with the alcohol amine solution [36]. Other important empirical correlations used in this model are shown in the following equations.

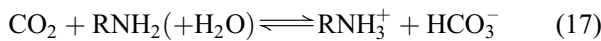
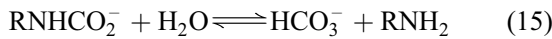
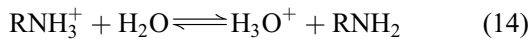
$$H_{CO_2,amine} = 3.31 \times 10^5 \times (5.52 + 0.7C_{MEA}) \times \exp\left(\frac{-1926}{T}\right), \quad [37] \quad (10)$$

$$D_{N_2O,amine} = (50.7 + 8.65C_{MEA} + 2.78C_{MEA}^2) \times 10^{-7} \times \exp\left(\frac{-2371 - 93.4C_{MEA}}{T}\right), \quad [38] \quad (11)$$

$$D_{CO_2,amine} = 0.464 \times \exp\left(\frac{252}{T}\right) \times D_{N_2O,amine}. \quad [39] \quad (12)$$

The calculation of this model requires various component concentrations, such as CO₂ concentration. Obtaining these parameters through complex chemical calculations is challenging to real-time calculation of dynamic models. In order to reduce the computational expense, the chemical reaction is simplified in this study. Assuming reaction rate is much greater than mass transfer rate, the CO₂ concentration can be calculated by chemical equilibrium constant.

Primary and secondary amines absorb CO₂ to form amino carbonates, while tertiary and hindered amines form bicarbonates. The main chemical reactions occurring in the liquid phase are shown in following equations.



Amine selection and its characteristics decide the way hybrid modeling physical mechanism and chemical reactions in a carbon dioxide capture process. Change of amine would lead to a complete change of the model. Only monoethanolamine is selected in this study since its model had been developed on Aspen Plus [31]. It's reaction expression with CO₂ is shown in Eq. (16). The equilibrium constant expression of the above reaction is as follows, and parameters are shown in Table 1.

$$\ln K_i = A_i + \frac{B_i}{T} + C_i \ln T + D_i T, \quad (18)$$

where K_i is the equilibrium constant, T is the liquid temperature, and the values of the four constants A_i , B_i , C_i , and D_i are listed in Table 1.

Ignoring other reactions, the reaction of monoethanolamine absorbing CO₂ can be approximated as a combination of Reactions 14–16. In this basis, reaction equilibrium constant can be calculated by K_{14} , K_{15} , K_{16} . The fitted expression is calculated by

$$\ln K = \ln K_{14} - \ln K_{15} - \ln K_{16} + E_k, \quad (19)$$

where E_k is a constant added to correct the error introduced by simplifying reactions. We believe that the influence of temperature has been considered in the equilibrium constant. Setting the CO₂ load in Aspen Plus from 0.05–0.46 [31], we calculated the CO₂ concentration in the monoethanolamine solution, where the monoethanolamine mass fraction is 30%, the temperature is 338 K. Fitting the constant E according to the Aspen Plus data, the reaction equilibrium constant is obtained. As shown in Fig. 2, we believe this fitted formula is sufficient to meet the accuracy requirements of CO₂ concentration calculation.

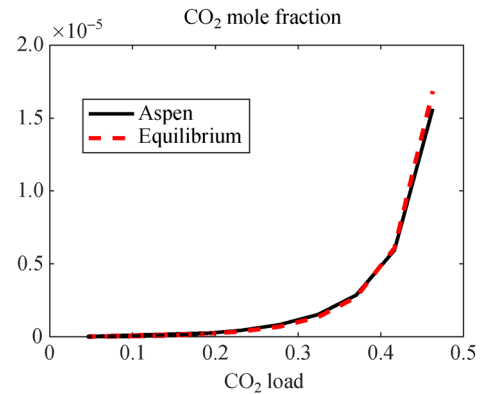


Fig. 2 Fitting results of CO₂ mole fraction.

Table 1 Parameters of the main chemical reaction for monoethanolamine to absorb CO₂

Reaction No.	A	B	C	D	$T/^\circ C$	Ref.
14	231.456	-12092.1	-36.7816	0	0–50	[40]
15	-4.90737	-6166.116	0	-0.000985	0–225	[41]
16	0.030669	-2275.19	0	0	0–225	[42]

Apart from the CO₂ absorption and desorption, the evaporation and condensation of H₂O greatly affect the temperature distribution and cannot be ignored. In this paper, considering temperature, H₂O mole fraction and chemical system as dominant factors, the empirical correlations of saturated H₂O vapor pressure is fitted, in which chemical system is represented by CO₂ load. The fitted expression is shown below, and the result is shown in Fig. 3. Compared with the data of Aspen Plus, the accuracy is sufficient for calculation.

$$P_{\text{H}_2\text{O}}^* = 0.0157e^{(0.0423T - 0.367load^5)} x_{\text{H}_2\text{O}}. \quad (20)$$

Main physical parameters of gas and liquid, such as density, viscosity and heat capacity, etc., are fitted according to the Aspen Plus data. Thus, the above formula can be programmed under a universal platform and language to calculate physical diffusion and chemical reactions

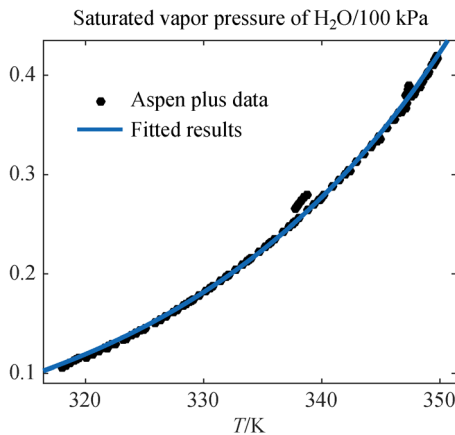


Fig. 3 Fitting results of saturated vapor pressure of H₂O.

2.2 Modeling of packed column

The plug flow reactor (PFR) model is a common way to represent packed columns [43], which assuming that the distribution of radial temperature, concentration, and velocity are consistent. In this basis, the packed column can be divided into multiple control volume along the height, which can be described by specific energy and mass conservation equations.

For the mass conservation, in the liquid control volume with a volume of $dV_1 = \varepsilon S dz$, the total molar change of the substance can be expressed as follows:

$$\Delta n_1 = \Delta N_1 \varepsilon S dt + a_{\text{eff}} dt \sum J_{i,\text{gl}}, \quad (21)$$

where ε represents the porosity, S represents the flow in and out areas of the control volume, a_{eff} represents the effective gas-liquid area, and $J_{i,\text{gl}}$ is the mass transfer

flux of component i through the gas-liquid interface ($\text{mol}/(\text{m}^2 \cdot \text{s}^{-1})$). When the control volume becomes infinitely small, the above formula can be transformed into a differential formula:

$$\frac{\partial C_1}{\partial t} = \frac{\partial N_1}{\partial z} + \frac{a_{\text{pck}}}{\varepsilon} \sum J_{i,\text{gl}}, \quad (22)$$

$$\frac{a_{\text{gl}}}{a_{\text{p}}} = 1 - \exp \left[-1.45 \left(\frac{\sigma_{\text{c}}}{\sigma_{\text{L}}} \right)^{0.75} \left(\frac{\rho_1 u_1}{a_{\text{p}} \mu_1} \right)^{0.1} \left(\frac{u_1^2 a_{\text{p}}}{g} \right)^{-0.05} \left(\frac{\rho_1 u_1^2}{\sigma_{\text{L}} a_{\text{p}}} \right)^{0.2} \right], \quad (23)$$

among which, a_{pck} is the effective interface area. a_{pck} is calculated by the empirical Eq. (23) [34]. The above formula is also applicable to the gas phase.

As for the energy conservation, ignoring other heat, the energy change inside the control volume is mainly determined by chemical reaction, heat flow, heat transfer between gas and liquid. The energy conservation equation and the differential formula for the control volume can be calculated by

$$\Delta \tilde{E}_1 = \Delta \tilde{Q}_1 \varepsilon h_1 S dt + a_{\text{eff}} dt \times q_{\text{cond}} + Q_{\text{rea}}, \quad (24)$$

$$\frac{\partial \tilde{E}_1}{\partial t} = \frac{\partial \tilde{Q}_1}{\partial z} + \frac{a_{\text{pck}}}{\varepsilon h_1} \times q_{\text{cond}} + q_{\text{rea}}, \quad (25)$$

where q_{cond} is the heat flux through conduction, q_{rea} is the heat flux generated by reaction, condensation and evaporation.

In addition to mass and energy conservation, the liquid flow between the control volume also deeply affects the dynamic behavior since the liquid velocity is much slower than gas side. In this study, the liquid transportation is calculated by liquid holdup. At a certain spray rate, the total liquid holdup is equal to the dynamic liquid holdup [44], which can be calculated by [45]:

$$h_{1,0} = 0.555 \left(U_1^2 \frac{a_{\text{p}}}{g \varepsilon^{4.65}} \right)^{1/3}. \quad (26)$$

Obtaining the holdup capacity, the liquid flowing to next stage $N_{1(t,z)}$ is equal to the liquid in the stage $V_{1(t,z)}$ minus the liquid holdup capacity $H_{1(t,z)}$. Expressions are as follows:

$$V_{1(t,z)} = V_{1(t-1,z)} + N_{1(t-1,z+1)}, \quad (27)$$

$$N_{1(t,z)} = V_{1(t,z)} - H_{1(t,z)}. \quad (28)$$

Thus, the above packed column models can be calculated and integrated with other unit models.

2.3 Modeling of heat exchanger

In the PCC plant, heat exchanger, condensation unit and cooler are also indispensable. Briefly modeled by shell and tube heat exchanger model, all these heat exchange components are added in whole process model. In this basis, the temperature change of liquid flowing out of heat exchanger is calculated by Eq. (29). The heat exchange through the wall can be calculated by the logarithmic temperature difference. Expressions are as follows:

$$\frac{dT_H^O}{dt} = -\frac{\dot{V}}{V^h} \frac{\partial T_g}{\partial L} + \frac{\dot{Q}}{C_p V^h}, \quad (29)$$

$$\dot{Q} = H \times 2\pi r_O \times L \times \frac{\Delta T_{in} - \Delta T_{out}}{\ln\left(\frac{\Delta T_{in}}{\Delta T_{out}}\right)}. \quad (30)$$

In addition, assuming pump power only changes the pressure, the pump model is simplified. The liquid storage tank model is also established as a normal tank. On the basis of these mathematical unit models, the dynamic whole process PCC model can be integrated and built on a universal platform and language.

Mixed programming by COM components, calculation program is written on MATLAB, and the user's interface is established on LabVIEW. The dynamic simulator of PCC plant is established. Even delayed by the communication between MATLAB and LabVIEW, this simulator still could achieve real-time simulation.

2.4 Steady state validation

In order to validate the model, operational data of a demonstration capture process at the University of Texas at Austin (48 cases, 24 operating conditions) are used. The inputs of Austin PCC plant are shown in Table 2 [46]. Inputting these data above into the model for calculation, CO₂ captures rate under different working conditions are obtained (scattered point), and compared with the experimental data (straight line). Results are shown in Fig. 4. Through the comparison of CO₂ capture rate, it can be observed that the calculation capture rate is distributed along the experimental capture rate. The relative average error between predicted capture rate and actual value is

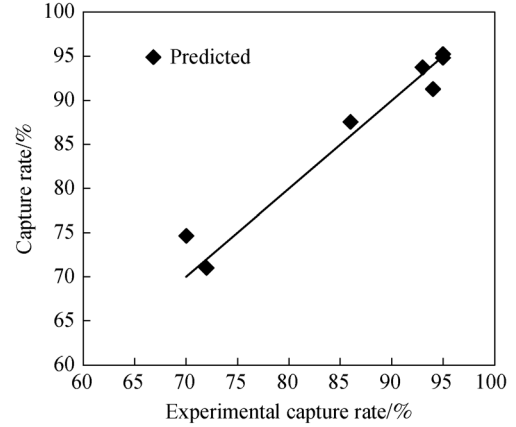


Fig. 4 Steady state validation.

4.3%, which indicated that the accuracy meets demand of simulation. In subsequent studies, as more experimental data are obtained, the model can be modified to improve the accuracy.

2.5 Dynamic simulation

Model outputs during dynamic transition are compared with data of a demonstration PCC pilot plant at Heilbronn, in which the flue gas increases by 30 percent, and the plant takes approximately 4 h to bring the reboiler back to a 90 percent capture rate. In this study, we conducted the similar dynamic operation as Heilbronn plant [18], in which case 40 input is adopted (90% capture rate), and the flue gas flow rate suddenly increases by 30% at 20000 s. In order to return to 90% capture rate, the reboiler power was increased by 12% synchronously. Figure 5 displayed the dynamic response of capture rate, which takes nearly 15000 s to recovery. Qualitatively, in terms of response time and amplitude, the results are consistent with the trend of the PCC pilot plant at Heilbronn.

3 Impact analysis of operating parameters

Flexible operation is based on the understanding of the performance of various operating parameters. In order to guide the subsequent optimized operation of PCC plant,

Table 2 Input data for working conditions of experimental PCC plant

Case No.	25	28	30	32	36	40	43
Lean amine temperature/K	313	313	313	314	313	313	313
Absorber inlet gas temperature/K	328	321	325	320	326	329	327
Lean amine CO ₂ loading	0.278	0.29	0.284	0.279	0.284	0.229	0.231
Y CO ₂	0.166	0.165	0.166	0.177	0.175	0.168	0.16
Amine rate/(mol·s ⁻¹)	72.87	57.47	38.43	28.49	29.96	58.17	27.58
Absorber gas rate/(mol·s ⁻¹)	6.81	6.96	6.87	3.49	3.50	6.79	6.83

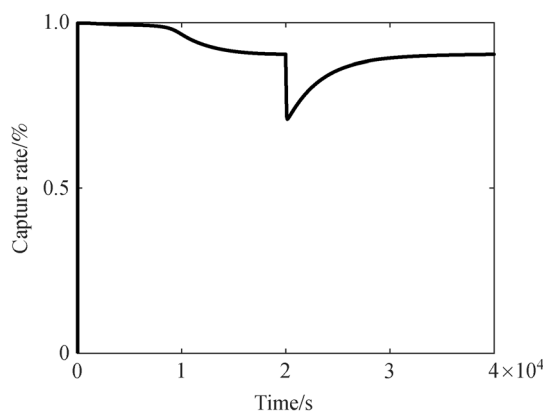


Fig. 5 Dynamic changes of model capture rate (Star-up, sudden increase in smoke).

performances of various design and operating parameters are studied.

3.1 Gas-liquid ratio

Gas-liquid ratio greatly affects capture rate when the flue gas flow rate and reboiler power remain constant. Based on input data of case 25, the effect of gas-liquid ratio is studied by only changing the monoethanolamine solution flow rate of absorber. When the steady state is reached, the CO₂ capture rate and the internal temperature distribution of absorber at four different amine flow rate are obtained and shown in Fig. 6. Figure 6(a) presents the capture rate under different amine flow rate. Under a certain gas flow rate, increasing the amine flow rate can effectively increase capture rate until capture rate is too high, such as over 95%, since the CO₂ partial pressure is too low to drive the absorption. Figure 6(b) presents the temperature distribution in absorber. As the amine flow rate increases, the temperature difference between control volumes becomes smaller, and the highest temperature of the absorber gradually moves to the outlet of solution. This discrepancy in the temperature distribution is due to the effect that larger solution flow will reduce the temperature difference between control volumes. In addition, the temperature is raised along the height by H₂O condensation and CO₂ absorption. Thus, controlling the gas-liquid ratio will help achieve the capture target under affordable expense in the operation of PCC plant.

3.2 Reboiler power

The CO₂ desorption was greatly determined by reboiler in which steam is generated to bring heat to the absorbent and dilute the released CO₂. The 60% working condition in Aspen Plus was adopted as the benchmark while other inputs remain unchanged besides the reboiler power. The CO₂ desorption rate and internal parameter distribution are

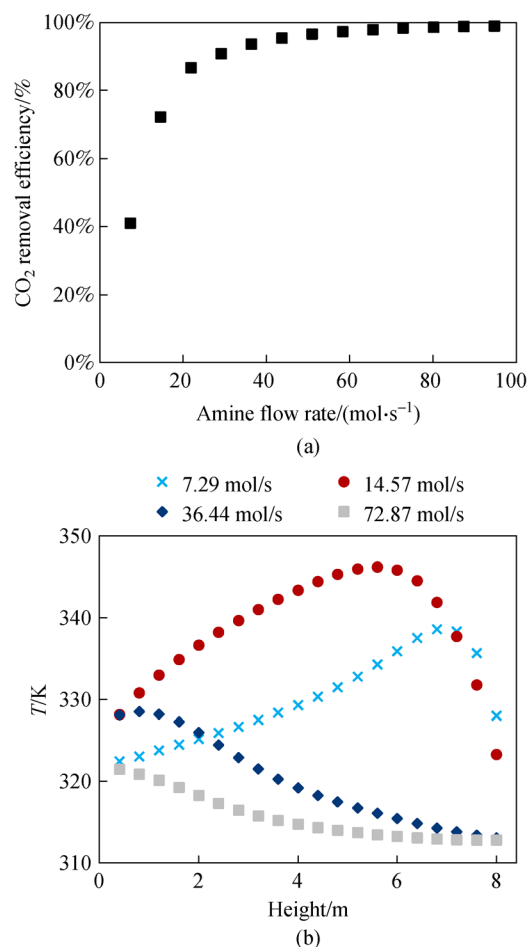


Fig. 6 PCC performance under different amine solution flow. (a) CO₂ capture rate under different amine flow rates; (b) Temperature distribution inside absorber under four different amine flow rates.

shown in Fig. 7. As shown in Fig. 7, it can be observed that increasing the reboiler power can effectively improve the desorption rate when the power of reboiler is low. Since greater reboiler power will evaporate more H₂O vapor, water vapor will dilute CO₂ in gas phase while providing energy for desorption, resulting in an increase in the desorption rate. In this basis, PCC plant can increase the reboiler power to reduce the CO₂ load of rich liquid, thereby increasing the capture rate of plant.

3.3 Desorber pressure

The high pressure in the desorber helps to condense H₂O, but it also hinders the desorption of CO₂ by increasing the partial pressure. In this study, setting desorber pressure from 105 to 420 kPa, the influence of desorber pressure on desorption is analyzed. The results are shown in Fig. 8. As shown in Fig. 8, we can conclude that the condensation of H₂O increases under higher desorber pressure, which provides more energy for desorption and leads to an

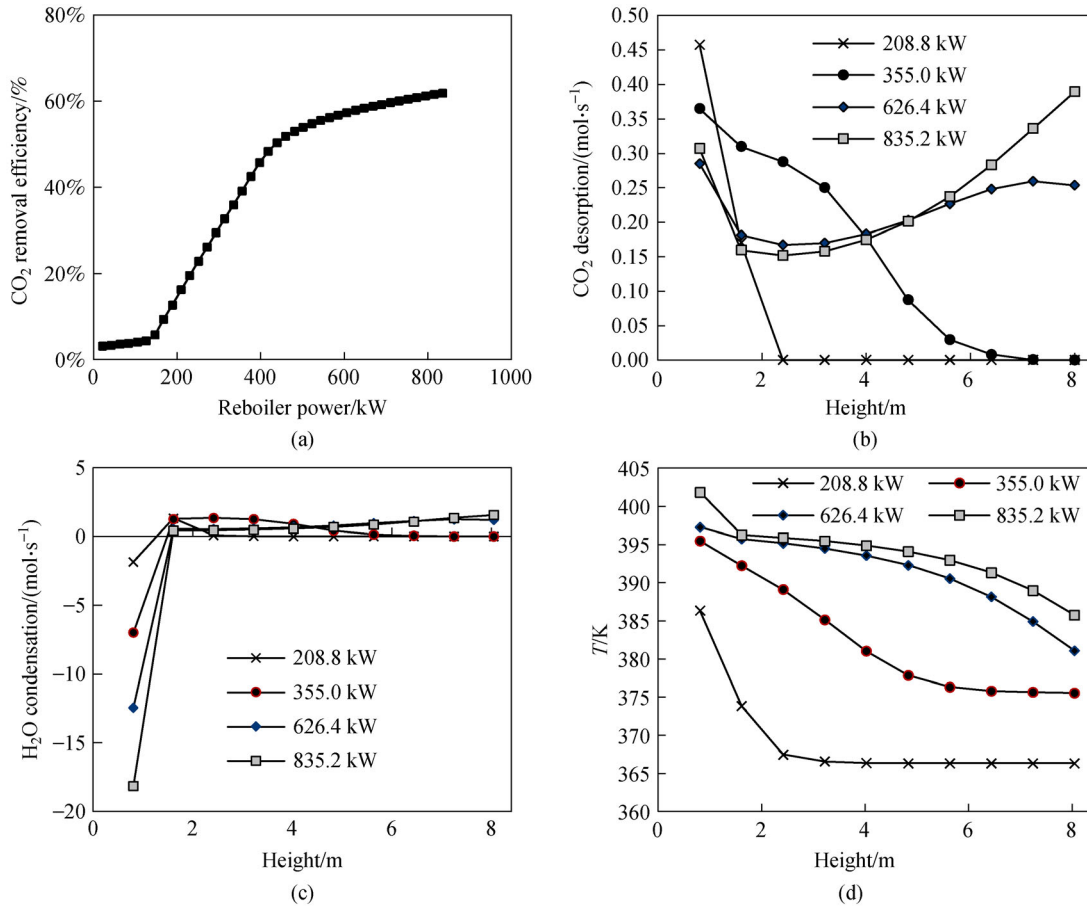


Fig. 7 Desorption under different reboiler power. (a) CO₂ removal efficiency inside desorber under different reboiler power; (b) CO₂ desorption distribution; (c) H₂O condensation distribution; (d) Temperature distribution inside desorber under four different reboiler power.

increase in CO₂ desorption rate. When desorber pressure is too high, desorption will mainly occur at the inlet and outlet stage of monoethanolamine solution due to massive condensation of water in the middle stage. Higher pressure can easily achieve higher temperature to improve the desorption effect, but the compression work introduced by higher pressure should also be considered.

3.4 Tower height

The packed column provides gas-liquid contact area for mass transfer, which is determined by tower height when the packing material and tower diameter are fixed. In this study, the case 40 working condition of Austin plant was adopted as benchmark. Input monoethanolamine solution and flue gas flow are changed from 0.5 to 1.5 times, and the tower height was set from 0.5 to 40 m. The capture rate under different tower height and flow rate are obtained and shown in Fig. 9. As shown in Fig. 9, the CO₂ capture rate gradually increases as the tower height increases under the same flow input. When the gas-liquid contact area is large enough, the capture benefit brought by the tower height

will gradually weaken. In addition, the gas-liquid contact area required for different flue gas flow to achieve the same capture target is different. The simulation reveals that tower height should be optimal designed according to the power plant's emission and capture target in the design of PCC plant.

3.5 Combination of solution flow rate and reboiler power

As discussed in above simulations, monoethanolamine solution flow rate, reboiler power, desorber pressure and tower height all have a significant impact on PCC plant's capture and desorption performance, among which monoethanolamine solution flow rate is the easiest parameter to change during operation. Optimizing the combination of operating parameters can achieve the same capture rate under different reboiler energy consumption. In this study, the capture rate is set to 90% and desorber pressure remains 210 kPa at the tower height of 10 and 15 m, thus the CO₂ capture rate and the lean load of PCC plant are functions of the monoethanolamine solution flow rate and the reboiler power: $a = f_1(\text{Flow rate}, \text{Reboiler power})$, lean load =

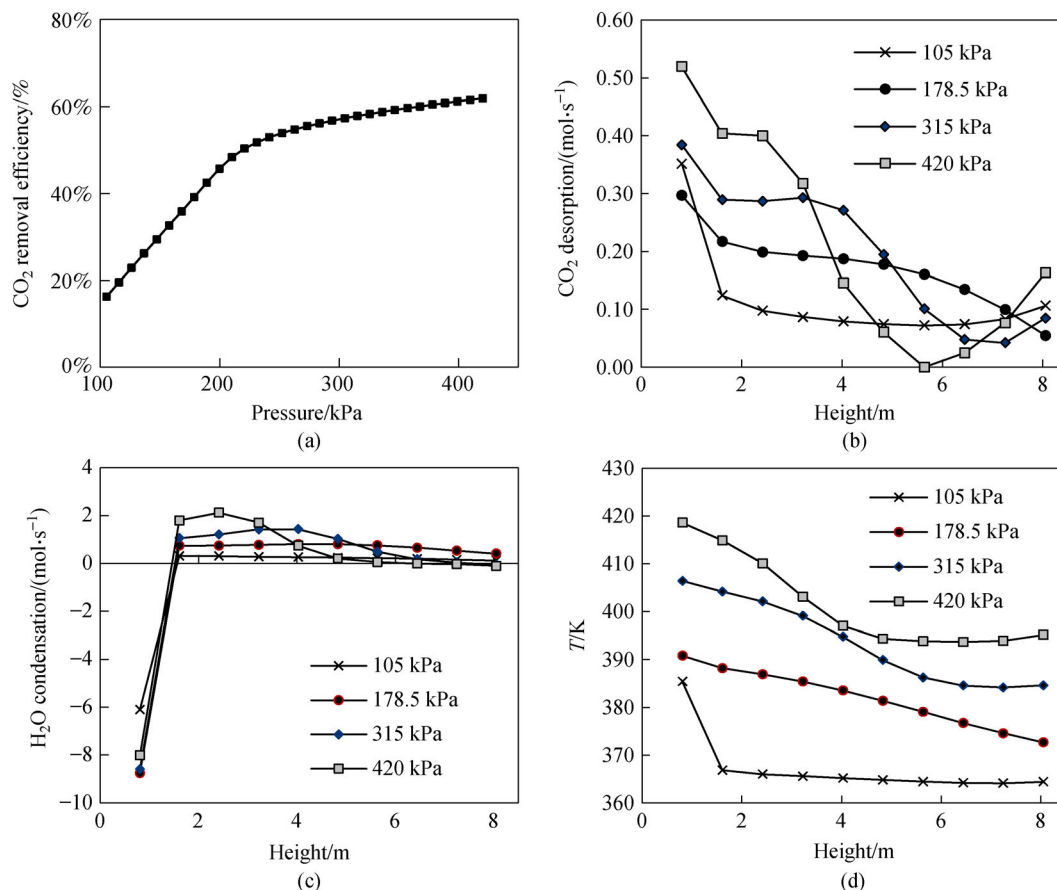


Fig. 8 Desorption under different pressure. (a) CO₂ removal efficiency under different desorber pressure; (b) CO₂ desorption distribution; (c) H₂O condensation distribution; (d) Temperature distribution inside desorber under four different desorber pressure.

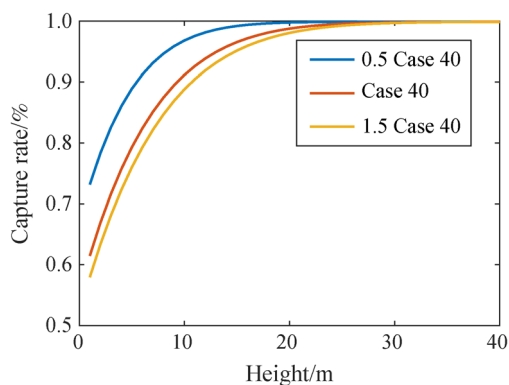


Fig. 9 CO₂ capture rate under different tower heights and flow rates.

$f_2(\text{Flow rate, Reboiler power})$ These working conditions are obtained and illustrated in Fig. 10.

Under a certain tower height, a larger monoethanolamine flow rate will allow PCC plant to achieve the same capture rate under a higher lean liquid CO₂ load. The reboiler power has a local/global minimum under a certain

lean liquid load due to the trade-off between monoethanolamine solution heating and H₂O evaporation heat. In actual operation, when tower height, solution composition and flue gas input parameters are fixed, the solution flow rate can be optimized to reduce the reboiler power while maintaining the same capture rate. As for different height shown in Figs. 10(a,c), the local or global optimal solution depends on the equipment. Higher tower height can fully absorb and desorb, thereby reducing the energy consumption of reboiler, but the increase in investment costs should also be considered.

4 Conclusions and outlook

In this manuscript, a hybrid PCC modelling approach is presented. The model is capable of online simulation of start-up and shutdown processes, as well as regular operation. The model is validated by steady data from the literature, and is used to study impacts of various design and operating parameters. Results indicate that gas-liquid ratio, reboiler power, desorber pressure, and tower height have large impacts on performance of a PCC plant,

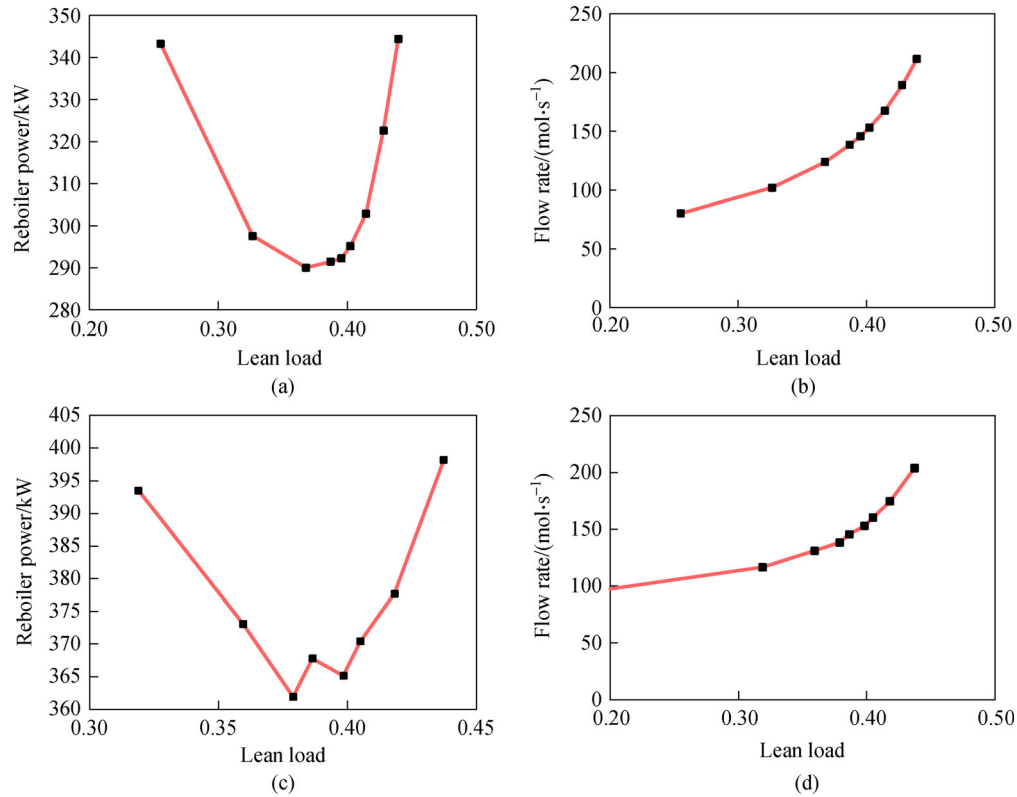


Fig. 10 Working conditions (90% capture rate) under different parameters. (a) Reboiler power under different lean load (15 m); (b) amine flow rate under different lead load (15 m); (c) reboiler power under different lean load (10 m); (d) amine flow rate under different lead load (10 m).

and provide directions for optimizing these key parameters.

Further studies could focus on dynamic validation and response of a PCC plant. For this purpose, dynamic operating data should be obtained to validate and modify the model. Additionally, the model could be integrated with a power plant model, together with its control system, for the purpose of online analysis and diagnosis of operation flexibility.

Acknowledgements This study was support by The National Key Research and Development of China (Grant No. 2019YFE0100100), Shanxi Key Research and Development Program (Grant No. 201603D312001), the National Natural Science Foundation of China (Grant No. 71690245), and the Phase III Collaboration between BP and Tsinghua University.

References

- Hanak D P, Manovic V. Linking renewables and fossil fuels with carbon capture via energy storage for a sustainable energy future. *Frontiers of Chemical Science and Engineering*, 2020, 14(3): 453–459
- Mumford K A, Yue W U, Smith K H, Stevens G W. Review of solvent-based carbon-dioxide capture technologies. *Frontiers of Chemical Science and Engineering*, 2015, 9(2): 125–141
- Lew D, Brinkman G, Kumar N, Besuner P, Agan D D, Lefton S. Impacts of wind and solar on emissions and wear and tear of fossil-fueled generators. In: 2012 IEEE Power and Energy Society General Meeting. San Diego: IEEE, 2012, 1–8
- Guido G D, Compagnoni M, Pellegrini L A, Rossetti H. Mature versus emerging technologies for CO₂ capture in power plants: Key open issues in post-combustion amine scrubbing and in chemical looping combustion. *Frontiers of Chemical Science and Engineering*, 2018, 12(2): 315–325
- Wall T F. Combustion processes for carbon capture. *Proceedings of the Combustion Institute*, 2007, 31(1): 31–47
- Cohen S M, Rochelle G T, Webber M E. Optimal operation of flexible post-combustion CO₂ capture in response to volatile electricity prices. *Energy Procedia*, 2011, 4: 2604–2611
- Wu X, Wang M, Liao P, Shen J, Li Y. Solvent-based post-combustion CO₂ capture for power plants: a critical review and perspective on dynamic modelling, system identification, process control and flexible operation. *Applied Energy*, 2020, 257: 257–113941
- Treybal R E. Adiabatic gas absorption and stripping in packed towers. *Industrial & Engineering Chemistry*, 1969, 61(7): 36–41
- Kenig E Y, Schneider R, Górak A. Reactive absorption: optimal process design via optimal modelling. *Chemical Engineering Science*, 2001, 56(2): 343–350
- Kvamsdal H M, Jakobsen J P, Hoff K A. Dynamic modeling and

- simulation of a CO₂ absorber column for post-combustion CO₂ capture. *Chemical Engineering and Processing*, 2009, 48(1): 135–144
11. Jayarathna S A, Lie B, Melaaen M C. Dynamic modelling of the absorber of a post-combustion CO₂ capture plant: modelling and simulations. *Computers & Chemical Engineering*, 2013, 53: 178–189
 12. Kvamsdal H M, Hillestad M. Selection of model parameter correlations in a rate-based CO₂ absorber model aimed for process simulation. *International Journal of Greenhouse Gas Control*, 2012, 11: 11–20
 13. Jayarathna S A, Lie B, Melaaen M C. NEQ rate based modeling of an absorption column for post combustion CO₂ capturing. *Energy Procedia*, 2011, 4(1): 1797–1804
 14. Ziaii S, Rochelle G T, Edgar T F. Dynamic modeling to minimize energy use for CO₂ capture in power plants by aqueous monoethanolamine. *Industrial & Engineering Chemistry Research*, 2009, 48(13): 6105–6111
 15. Enaasen N, Tobiesen A, Kvamsdal H M, Hillestad M. Dynamic modeling of the solvent regeneration part of a CO₂ capture plant. *Energy Procedia*, 2013, 37(1): 2058–2065
 16. Lawal A, Wang M, Stephenson P, Koumpouras G, Yeung H. Dynamic modelling and analysis of post-combustion CO₂ chemical absorption process for coal-fired power plants. *Fuel*, 2010, 89(10): 2791–2801
 17. Jayarathna S A, Lie B, Melaaen M C. Amine based CO₂ capture plant: dynamic modeling and simulations. *International Journal of Greenhouse Gas Control*, 2013, 14(5): 282–290
 18. Wellner K, Marx-Schubach T, Schmitz G. Dynamic behavior of coal-fired power plants with post combustion CO₂ capture. *Industrial & Engineering Chemistry Research*, 2016, 55(46): 12038–12045
 19. Dutta R, Nord L O, Bolland O. Selection and design of post-combustion CO₂ capture process for 600 MW natural gas fueled thermal power plant based on operability. *Energy*, 2017, 121: 643–656
 20. Montañés R M, GarDarsdóttir S Ó, Normann F, Johnsson F, Nord L O. Demonstrating load-change transient performance of a commercial-scale natural gas combined cycle power plant with post-combustion CO₂ capture. *International Journal of Greenhouse Gas Control*, 2017, 63: 158–174
 21. Wu X, Wang M, Shen J, Li Y, Lawal A, Lee K Y. Reinforced coordinated control of coal-fired power plant retrofitted with solvent based CO₂ capture using model predictive controls. *Applied Energy*, 2019, 238: 495–515
 22. He X, Lima F V. Development and implementation of advanced control strategies for power plant cycling with carbon capture. *Computers & Chemical Engineering*, 2018, 121: 497–509
 23. Zhang Q, Turton R, Bhattacharyya D. Nonlinear model predictive control and H-infinity robust control for a post-combustion CO₂ capture process. *International Journal of Greenhouse Gas Control*, 2019, 82: 138–151
 24. Madeddu C, Errico M, Baratti R. Process analysis for the carbon dioxide chemical absorption-regeneration system. *Applied Energy*, 2018, 251: 532–542
 25. Moullec Y L, Neveux T, Azki A A, Chikukwa A, Hoff K A. Process modifications for solvent-based post-combustion CO₂ capture. *International Journal of Greenhouse Gas Control*, 2014, 31: 96–112
 26. Dowell N M, Shah N. The multi-period optimisation of an amine-based CO₂ capture process integrated with a super-critical coal-fired power station for flexible operation. *Computers & Chemical Engineering*, 2015, 74: 169–183
 27. Dowell N M, Shah N. Dynamic modelling and analysis of a coal-fired power plant integrated with a novel split-flow configuration post-combustion CO₂ capture process. *International Journal of Greenhouse Gas Control*, 2014, 27: 103–119
 28. Gaspar J, Jorgensen J B, Fosbol P L. Control of a post-combustion CO₂ capture plant during process start-up and load variations. *IFAC-PapersOnLine*, 2015, 48(8): 580–585
 29. Marx-Schubach T, Schmitz G. Modeling and simulation of the start-up process of coal fired power plants with post-combustion CO₂ capture. *International Journal of Greenhouse Gas Control*, 2019, 87: 44–57
 30. Åkesson J, Laird C D, Lavedan G, Prölb K, Tummescheit H, Velut S, Zhu Y. Nonlinear model predictive control of a CO₂ post combustion absorption unit. *Chemical Engineering & Technology*, 2012, 35(3): 445–454
 31. Jin H, Liu P, Li Z. Energy-efficient process intensification for post-combustion CO₂ capture: a modeling approach. *Energy*, 2018, 158: 471–483
 32. Harun N, Nittaya T, Douglas P L, Croiset E, Ricardez-Sandoval L A. Dynamic simulation of MEA absorption process for CO₂ capture from power plants. *International Journal of Greenhouse Gas Control*, 2012, 10: 295–309
 33. Lyu B H. Mass transfer-reaction mechanism of CO₂ absorption in MEA/ionic liquid mixed aqueous solution. Dissertation for the Doctoral Degree. Zhejiang: Zhejiang University, 2014, 59–60
 34. Onda K, Takeuchi H, Okumoto Y. Mass transfer coefficients between gas and liquid phases in packed columns. *Journal of Chemical Engineering of Japan*, 1968, 1(1): 56–62
 35. Danckwerts P V, Lannus A. Gas-liquid reactions. *Journal of the Electrochemical Society*, 1970, 117(10): 369C
 36. Ramachandran N, Aboudheir A, Idem R, Tontiwachwuthikul P. Kinetics of the absorption of CO₂ into mixed aqueous loaded solutions of monoethanolamine and methyldiethanolamine. *Industrial & Engineering Chemistry Research*, 2006, 45(8): 2608–2616
 37. Saha A K, Bandyopadhyay S S, Biswas A K. Solubility and diffusivity of nitrous oxide and carbon dioxide in aqueous solutions of 2-amino-2-methyl-1-propanol. *Journal of Chemical & Engineering Data*, 1993, 38(1): 78–82
 38. Versteeg G F, Van Swaaij W P M. Solubility and diffusivity of acid gases (carbon dioxide, nitrous oxide) in aqueous alkanolamine solutions. *Journal of Chemical & Engineering Data*, 1988, 33(1): 29–34
 39. Ko J J, Tsai T C, Lin C Y, Wang H M, Li M H. Diffusivity of nitrous oxide in aqueous alkanolamine solutions. *Journal of Chemical & Engineering Data*, 2001, 46(1): 160–165
 40. Edwards T J, Maurer G, Newman J, Prausnitz J M. Vapor-liquid equilibria in multicomponent aqueous solutions of volatile weak electrolytes. *AIChE Journal*, 1978, 24(6): 966–976
 41. Bower V E, Robinson R A, Bates R G. Acidic dissociation constant and related thermodynamic quantities for diethanolammonium ion

- in water from 0 to 50 °C. *Journal of Research of the National Bureau of Standards*, 1962, 66(1): 71–75
42. Li H, Chen J. Thermodynamic model and process simulation of CO₂ absorption by monoethanolamine. *CIESC*, 2014, 65(1): 47–54
43. Gaspar J, Jørgensen J B, Fosbøl P L. A dynamic mathematical model for packed columns in carbon capture plants. In: 2015 European Control Conference (ECC). Linz: IEEE, 2015, 2738–2743
44. Bemer G G, Kalis G A J. New calculation method of liquid holding capacity and pressure drop in packed tower. *Guangxi Chemical Technology*, 1979, 1979(2): 55–63
45. Stichlmair J, Bravo J L, Fair J R. General model for prediction of pressure drop and capacity of countercurrent gas/liquid packed columns. *Gas Separation & Purification*, 1989, 3(1): 19–28
46. Jayarathna S A, Lie B, Melaaen M C. Development of a dynamic model of a post combustion CO₂ capture process. *Energy Procedia*, 2013, 37: 1760–1769